2D MoSe$_2$ Structures Prepared by Atomic Layer Deposition

Milos Krbal, Jan Prikryl, Raul Zazpe, Filip Dvorak, Filip Bures, and Jan M. Macak*

Here, we demonstrate the preparation of 2D MoSe$_2$ structures by the atomic layer deposition technique. In this work, we use ((CH$_3$)$_3$Si)$_2$Se as the Se precursor and Mo(CO)$_6$ or MoCl$_5$ as the Mo precursors. The X-ray photoelectron spectroscopy (XPS) analyses of the prepared samples have revealed that using the MoCl$_5$ precursor the obtained structure of MoSe$_2$ is nearly identical to the reference powder MoSe$_2$ sample while the composition of the sample prepared from Mo(CO)$_6$ contains a significant amount of oxygen atoms. Further inspection of as-deposited samples via scanning electron microscopy (SEM), X-ray diffraction (XRD), and Raman spectroscopy has disclosed that the MoSe$_2$ structure based on MoCl$_5$ is formed from randomly oriented well crystalline flakes with their size ≈100 nm in contrast to the Mo–Se–O compact film originating from Mo(CO)$_6$.

A few years ago, the success of graphene opened a door for a new class of chalcogenide materials with unique properties that can be applied in the semiconductor technology. This class is so-called 2D transition-metal dichalcogenides (TMDCs)[1–4] represented by a generic formula MX$_2$, where M is a IV–VI transition metal atom (IV – Ti and Zr; V – V and Nb; VI – Mo and W) and X is chalcogen (S, Se, or Te). They possess a layered crystal structure where triple layers in TMDCs (such as X-TM-X) are weakly coupled by van der Waals forces, which determine the 2D nature of the crystalline phases. In contrast to graphene, monolayers of 2D TMDC possess

Dr. M. Krbal, J. Prikryl, Dr. R. Zazpe, Dr. F. Dvorak, Dr. J. M. Macak
Faculty of Chemical Technology
Center of Materials and Nanotechnologies
University of Pardubice
Nam. Cs. Legii 565, 53002 Pardubice, Czech Republic
E-mail: jan.macak@upce.cz

Dr. F. Bures
Faculty of Chemical Technology
Institute of Organic Chemistry and Technology
University of Pardubice
Studentska 573, 53210 Pardubice, Czech Republic

Dr. J. M. Macak
Central European Institute of Technology
Brno University of Technology
Purkynova 123, 61200 Brno, Czech Republic

The ORCID identification number(s) for the author(s) of this article can be found under https://doi.org/10.1002/pssr.201800023.

a direct band gap[5] that is crucial for optoelectronic applications.[3] Additionally, the direct band gap can be easily tuned by either chemical composition[6,7] or external stimuli, such as external fields[1] or external pressure.[8,9] Next to the optoelectronic applications, where a monolayer planar structure is necessary to employ, a layer of standing flakes, which possesses a large surface area, can be used in fields of a hydrogen evolution,[10,11] a photodegradation of organic dyes[12] or as electrodes in Li ion batteries.[13,14]

In principle, TMDCs can be prepared in two ways, i.e., top-down and bottom-up techniques.[3] Top-down fabrication methods include mechanical and chemical exfoliation based on direct ultrasonication and ion intercalation whereas the bottom-up deposition methods, such as chemical vapor deposition (CVD) and atomic layer deposition (ALD) growth techniques, serve to fabricate large area layers with monolayer precision. MoS$_2$, a typical representative of TMDCs, has been widely studied for many applications. Recently, the possibility to employ ALD as a technique to grow MoS$_2$ has been reported. In these works (CH$_3$)$_2$S$_2$[15] or H$_2$S[16,17] were used as the S precursor and Mo(CO)$_6$,[15] MoCl$_5$[16] or Mo(thd)$_3$[17] as the Mo precursors. From the practical point of view, MoS$_2$ is even more interesting than MoS$_2$ since MoSe$_2$ possesses a higher electrical conductivity than MoS$_2$[18,19] which is extremely important in electrochemical applications such as solar cells, batteries, supercapacitors, and electrocatalysis.[19] To the best authors' knowledge, there is no report on 2D MoSe$_2$ films or flakes deposited by ALD.

To close this gap, we deposited MoSe$_2$ structures on fused silica substrates by ALD using ((CH$_3$)$_3$Si)$_2$Se as the Se precursor,[20,21] which has been recently developed for selenides, and the aforementioned Mo(CO)$_6$ or MoCl$_5$ as the Mo precursors to reveal the effect of Mo precursors on the MoSe$_2$ growth. The ALD growth was conducted under the same conditions except of the deposition temperatures which were 167 and 300 °C for Mo(CO)$_6$ and MoCl$_5$, respectively, since Mo(CO)$_6$ decomposes above 175 °C.[22] The quality of as-prepared films or flakes was subsequently inspected by X-ray photoelectron spectroscopy (XPS), scanning electron microscopy (SEM), X-ray diffraction (XRD), and UV-Vis spectrophotometry.

Results and Discussion: The compositional analyses of the as-prepared MoSe$_2$ structures deposited on fused silica substrates were performed by XPS. **Figure 1** shows XPS spectra for Mo 3d and Se 3d core levels of as-deposited MoSe$_2$ structures prepared by ALD using Mo(CO)$_6$ and MoCl$_5$ Mo precursors and compared to a MoSe$_2$ powder reference sample. It is obvious at a first sight that the composition of the sample prepared from Mo(CO)$_6$ is different from the sample prepared from MoCl$_5$ and the reference sample.
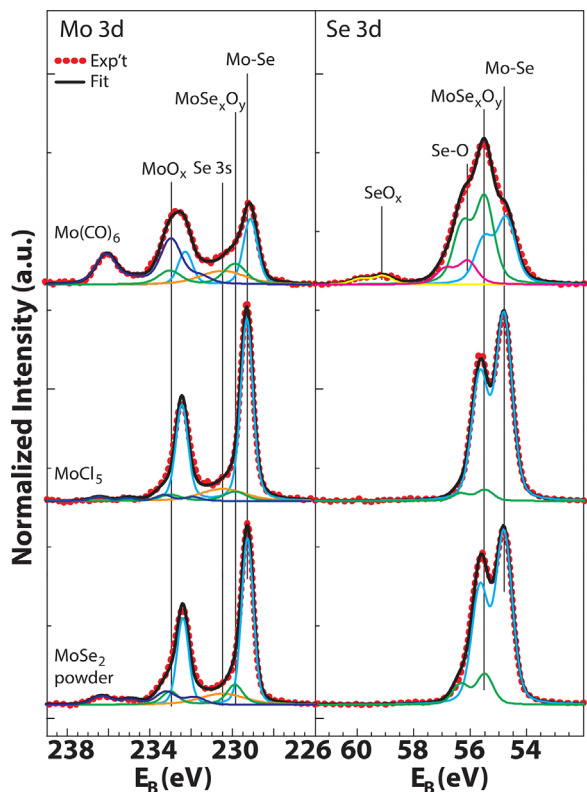
Figure 1. XPS spectra for Mo 3d (left) and Se 3d (right) of as-deposited MoSe$_2$ structures prepared by ALD using Mo(CO)$_6$ or MoCl$_5$ as Mo precursors and ((CH$_3$)$_3$Si)$_2$Se as the Se precursor. MoSe$_2$ powder sample is the reference material.

Table 1. Contribution of elements to XPS signal, %.

Elements	Mo	Se	C	O
Mo(CO)$_6$	16	25	21	38
MoCl$_5$	22	35	26	17
MoSe$_2$ powder	10	16	70	7

a field emission scanning electron microscope. The SEM image of MoSe$_2$ thin film deposited from Mo(CO)$_6$ unveiled that the surface of the fused silica substrate is evenly covered. However, no sign of typical crystalline structures of TMDCs such as plane triangles or standing flakes can be observed. On the other hand, MoSe$_2$ grown from MoCl$_5$ at 300 °C is formed from well evolved standing flakes with an average size of 100 nm attached to a thin underneath base layer. Larger magnification SEM top-view images of the same samples are shown in Figure S1, Supporting Information. Cross-sectional images of MoSe$_2$ flake layer (from the MoCl$_5$ precursor) are shown in Figure S2, Supporting Information and reveal thickness of the base layer on the scale of ≈10 nm. It is fair to point out that the ALD growth of MoSe$_2$ from the latter Mo precursor at 200 °C, which is comparable temperature to the former Mo precursor, led to the formation of small islands with unknown composition, as shown in
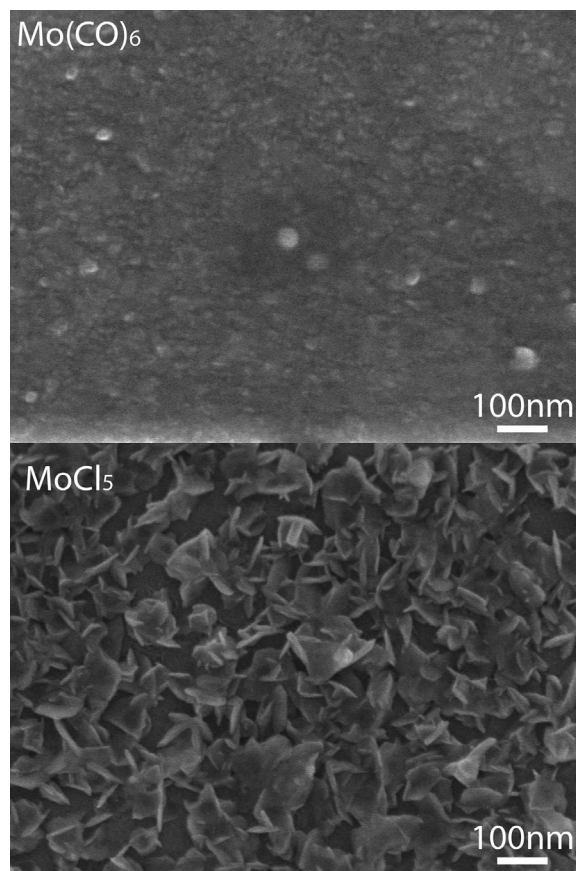
The deeper analysis of Mo 3d core levels disclosed that the XPS spectra of all samples are a mixture of Mo(IV)–Se (light blue) with the binding energy $E_B(3d_{5/2}) = 229.1$ eV,[23,24] Mo(IV)–Se/O (light green) with $E_B(3d_{5/2}) = 229.9$ eV,[25] Se 3s (orange) with $E_B(3s) = 230.5$ eV[25] and Mo(V/VI)–O (dark blue) with $E_B(3d_{5/2}) = 231.6$ eV/233 eV[26–28] (the MoO$_x$ components are drawn together for better clarity in Figure 1). The position of $E_B(3d_{5/2})$ for Mo(IV)–Se indicates 2H MoSe$_2$ phase.[29] The corresponding spin–orbit split doublets of Mo–Se and Mo–Se$_x$–O$_y$ depicting the Se^{2-} oxidation state with E_B 54.7 and 55.4 eV,[25] respectively, are identified in the Se 3d in Figure 1. Comparison of Mo 3d and Se 3d core levels for as prepared samples from different Mo precursors with the MoSe$_2$ reference sample clearly manifests that the composition of flakes of MoSe$_2$ deposited from MoCl$_5$ is nearly identical to the reference sample whereas a significant contribution of MoO$_x$ component can be found in the thin film grown from Mo(CO)$_6$. The strong oxidation of the latter sample is further corroborated with the presence of Se-oxide (magenta) with $E_B(3d_{5/2}) = 56.1$ eV[26,27] and Se-suboxide (yellow) with $E_B(3d_{5/2}) = 59.1$ eV[26,27] observed in Se 3d spectrum. No trace of elemental Se was detected in any samples. Based on the quantitative analysis of Mo 3d, Se 3d, and O 1s (not shown) spectral areas, the elemental ratio of Mo:Se:O corrected on sensitivity factors are written in **Table 1**.

Figure 2 demonstrates the morphology of as-deposited Mo-Se films (present uniformly on the whole area of fused silica substrates with the size of 2.5 × 1.5 cm) which was monitored by

Figure 2. SEM images of as-deposited MoSe$_2$ thin films or flakes, prepared by ALD using Mo(CO)$_6$ or MoCl$_5$, respectively, as Mo precursors and ((CH$_3$)$_3$Si)$_2$Se as the Se precursor.

Figure S3, Supporting Information along with SEM images of the $MoSe_2$ reference powder sample.

We studied the crystallinity of the films and flakes using XRD in grazing incidence geometry. We performed background subtraction using FullProf software package[30] to remove the XRD signal of the glass substrate. One can see from **Figure 3** that the XRD spectrum of the thin film deposited from $Mo(CO)_6$ contains a single peak at $2\theta = 14.4°$ in contrast to the XRD pattern of the $MoSe_2$ sample grown from $MoCl_5$ which is characterized by three peaks at $2\theta = 15.9°$, $2\theta = 36.95°$, and $2\theta = 66°$ corresponding to the (002), (100), and (110) planes of hexagonal $MoSe_2$.[31] In comparison with the reference powder sample, the positions of crystallographic planes of ALD $MoSe_2$ grown from $MoCl_5$ perfectly match with those of the reference sample which indicates that we have prepared well crystalline single phase of 2H $MoSe_2$. Regarding the structure of the ALD film prepared from $Mo(CO)_6$, the single peak is shifted toward lower 2θ than in pure $MoSe_2$. This shift can be attributed to the substitution of some Se by O within the $MoSe_2$ structure which is supported by the XPS analysis. Further, the intensity of the only one peak is four times lower comparing to the ALD $MoSe_2$ film prepared from $MoCl_5$, which might lead to the conclusion that the crystalline phase co-exists with the amorphous MoO_x phase.

Raman spectroscopy is a powerful tool to evaluate the quality of prepared TMDCs and their number of layers. We investigated the vibration modes of $MoSe_2$ fabricated from $Mo(CO)_6$ and $MoCl_5$ shown in **Figure 4**. Using an excitation wavelength of 532 nm, the $MoSe_2$ sample deposited from the $MoCl_5$ precursor consists of the characteristic out-of-plane A_{1g} mode at 241 cm^{-1} and the weak in-plane E^1_{2g} mode peaking at 287 cm^{-1} which is in excellent agreement with published Raman spectra of $MoSe_2$.[32,33] In contrast, $MoSe_2$ film prepared from $Mo(CO)_6$ contains peaks at 238, 256, 285, and 299 cm^{-1}. The latter vibration can be attributed to MoO_3.[34] The vibration at ≈ 285 cm^{-1} is presented in both $MoSe_2$ and MoO_3 phases.[32,35] Since vibrations at 238 and 256 cm^{-1} are close to pure $MoSe_2$ and MoO_3 we assign them to Mo–Se_x–O_y.

Figure 4. Raman spectra of as-deposited $MoSe_2$ structures prepared by ALD using $Mo(CO)_6$ (blue) or $MoCl_5$ (red) with out-of-plane (A_{1g}) and in-plane (E^1_{2g}) vibration modes.

Finally, we investigated optical properties of ALD $MoSe_2$ films or flakes. **Figure 5** shows absorbance spectra of ALD $MoSe_2$ structures deposited from both Mo precursors. One can see that excitons, which correspond to the splitting of the valence band by spin orbit coupling,[3,32] are generated only in the $MoSe_2$ sample deposited from the $MoCl_5$ precursor. Since the presence of excitons is associated with the crystal symmetry in Brillouin zone,[36] the observation of this phenomenon confirms as well the high crystalline quality of prepared $MoSe_2$ flakes using the $MoCl_5$ precursor. In the case of bulk $MoSe_2$, the A and B excitonic transitions at 300 K were localized at 1.54 and 1.81 eV.[37] On the other hand, it has been recently reported that the position of B excitonic feature for monolayered $MoSe_2$ was slightly shifted to lower photon energies in comparison with the bulk $MoSe_2$.[38] We found that A and B excitons for ALD $MoSe_2$ layer are positioned at 807 (1.54 eV) and 710 nm (1.75 eV) which are in good accordance to previously reported values for monolayered $MoSe_2$[38] indicating that the $MoSe_2$ deposited by
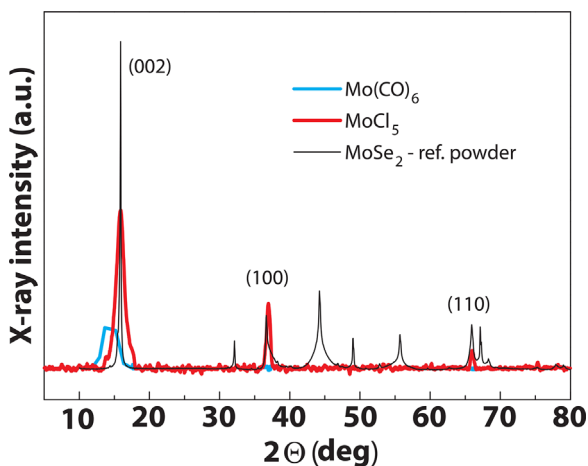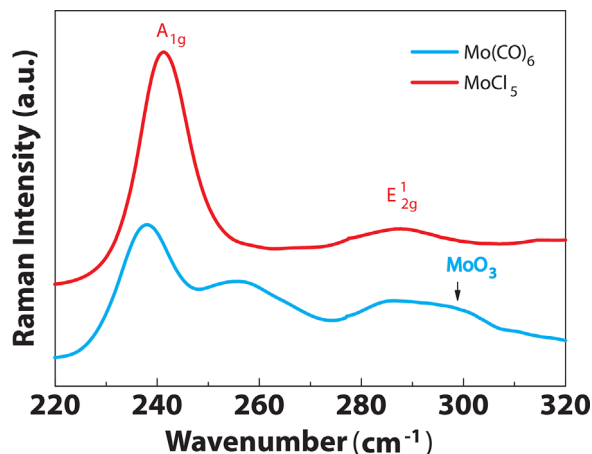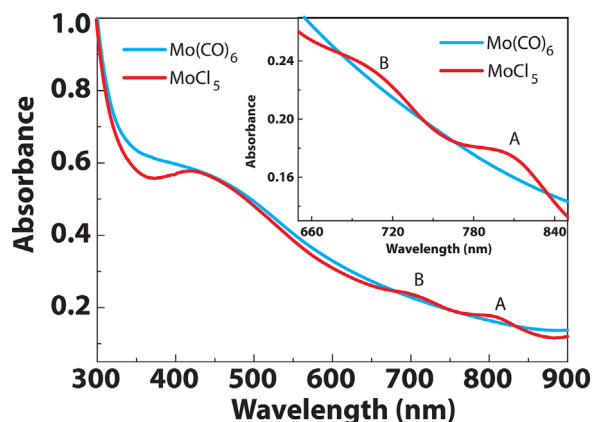
Figure 3. XRD patterns of as-deposited $MoSe_2$ structures prepared by ALD using $Mo(CO)_6$ (blue) or $MoCl_5$ (red). The black line represents $MoSe_2$ powder sample as the reference material.

Figure 5. Absorbance spectra of as-deposited $MoSe_2$ structures prepared by ALD using $Mo(CO)_6$ (blue) or $MoCl_5$ (red) as Mo precursors and $((CH_3)_3Si)_2Se$ as the Se precursor. The inserted figure shows the region of excitonic features labeled A and B.

ALD possesses 2D layered character rather than the bulk structure.

In conclusion, we have demonstrated the preparation of $MoSe_2$ structures by the ALD technique using $((CH_3)_3Si)_2Se$ and $Mo(CO)_6$ or $MoCl_5$ precursors. Upon characterization of as prepared materials by several techniques, we found that high quality crystalline $MoSe_2$ flakes can be obtained from the $MoCl_5$ precursor, in contrast to $MoSe_2$ films with MoO_x content obtained using $Mo(CO)_6$ precursor. We believe that the developed methodology can pave the way to advanced $MoSe_2$ structures with tailored properties and further prospective applications.

Supporting Information

Acknowledgments

Conflict of Interest

The authors declare no conflict of interest.

Keywords

[1] Q. H. Wang, K. Kalantar-Zadeh, A. Kis, J. N. Coleman, M. S. Strano, *Nat. Nanotechnol.* **2012**, *7*, 699.

[2] Z. M. Wang (Ed.), *MoS₂ Materials, Physics, and Devices*. Springer International Publishing, Switzerland **2014**.

[3] A. V. Kolobov, J. Tominaga, *Two-Dimensional Transition-Metal Dichalcogenides*. Springer Series in Materials Science, Springer International Publishing AG, Switzerland **2016**.

[4] K. F. Mak, J. Shan, *Nat. Photon.* **2016**, *10*, 216.

[5] B. Radisavljevic, A. Radenovic, J. Brivio, V. Giacometti, A. Kis, *Nat. Nanotechnol.* **2011**, *6*, 147.

[6] G. Wang, C. Robert, A. Suslu, B. Chen, S. Yang, S. Alamdari, I. C. Gerber, T. Amand, X. Marie, S. Tongay, B. Urbaszek, *Nat. Commun.* **2015**, *6*, 10110.

[7] Q. Feng, Y. Zhu, J. Hong, M. Zhang, W. Duan, N. Mao, J. Wu, H. Xu, F. Dong, F. Lin, C. Jin, C. Wang, J. Zhang, L. Xie, *Adv. Mater.* **2014**, *26*, 2648.

[8] Y. Y. Hui, X. Liu, W. Jie, N. Y. Chan, J. Hao, Y. T. Hsu, L. J. Li, W. Guo, S. P. Lau, *ACS Nano* **2013**, *7*, 7126.

[9] A. P. Nayak, Z. Yuan, B. Cao, J. Liu, J. Wu, S. T. Moran, T. Li, D. Akinwande, C. Jin, J. F. Lin, *ACS Nano* **2015**, *9*, 9117.

[10] X. Zhou, J. Prikryl, M. Krbal, J. M. Macak, P. Schmuki, *Electrochem. Commun.* **2017**, *82*, 112.

[11] L. Wang, Z. Sofer, J. Luxa, M. Pumera, *Adv. Mater. Interfaces* **2015**, *2*, 1500041.

[12] Y. Wu, M. Xu, X. Chen, S. Yang, H. Wu, J. Pan, X. Xiong, *Nanoscale* **2016**, *8*, 440.

[13] D. Ilic, K. Wiesener, W. Schneider, H. Oppermann, G. Krabbes, *J. Power Sources* **1985**, *14*, 223.

[14] N. A. Kyerementeng, N. Plylahan, A. C. S. dos Santos, L. V. Taveira, L. F. P. Dick, T. Djenizian, *Chem. Commun.* **2013**, *49*, 4205.

[15] Z. Jin, S. Shin, D. H. Kwon, S. J. Han, Y. S. Min, *Nanoscale* **2014**, *6*, 14453.

[16] L. K. Tan, B. Liu, J. H. Teng, S. Guo, H. Y. Low, K. P. Loh, *Nanoscale* **2014**, *6*, 10584.

[17] M. Mattinen, T. Hatanpää, T. Sarnet, K. Mizohata, K. Meiander, P. J. King, L. Khriachtchev, J. Risnen, M. Ritala, M. Leskelä, *Adv. Mater. Interfaces* **2017**, *4*, 1700123.

[18] D. Kong, H. Wang, J. J. Cha, M. Pasta, K. J. Koski, J. Yao, Y. Cui, *Nano Lett.* **2013**, *13*, 1341.

[19] A. Eftekhari, *Appl. Mater. Today* **2017**, *8*.

[20] V. Pore, T. Hatanpää, M. Ritala, M. Leskelä, *J. Am. Chem. Soc.* **2009**, *131*, 3478.

[21] T. Hatanpää, V. Pore, M. Ritala, M. Leskelä, *ECS Trans.* **2009**, *25*, 609.

[22] D. K. Nandi, S. K. Sarkar, *Appl. Mech. Mater.* **2014**, *492*, 375.

[23] S. Vishwanath, X. Liu, S. Rouvimov, P. C. Mende, A. Azcatl, S. McDonnell, R. M. Wallace, R. M. Feenstra, J. K. Furdyna, D. Jena, *2D Mater.* **2015**, *2*, 024007.

[24] B. B. Wang, M. K. Zhu, K. Ostrikov, R. W. Shao, K. Zheng, *J. Alloys Compd.* **2015**, *647*, 734.

[25] A. Azcatl, S. KC, X. Peng, N. Lu, S. McDonnell, X. Qin, F. de Dios, R. Addou, J. Kim, M. J. Kim, K. Cho, R. M. Wallace, *2D Mater.* **2015**, *2*, 014004.

[26] P. A. Spevack, N. S. McIntyre, *J. Phys. Chem. C* **1992**, *96*, 9029.

[27] J. Baltrusaitis, B. Mendoza-Sanchez, V. Fernandez, R. Veenstra, N. Dukstiene, A. Roberts, N. Fairley, *Appl. Surf. Sci.* **2015**, *326*, 151.

[28] S. McDonnell, A. Azcatl, R. Addou, C. Gong, C. Battaglia, S. Chuang, K. Cho, A. Javey, R. M. Wallace, *ACS Nano* **2014**, *8*, 6265.

[29] A. Ambrosi, Z. Sofer, M. Pumera, *Chem. Commun.* **2015**, *51*, 8450.

[30] J. Rodriguez-Carvajal, *Physica B* **1993**, *192*, 55.

[31] L. M. Kulikov, A. A. Semenov-Kobzar, L. G. Akselrud, T. A. Lobova, E. A. Bogachev, *Inorg. Mater.* **1992**, *28*, 397.

[32] P. Tonndorf, R. Schmidt, P. Böttger, X. Zhang, J. Börner, A. Liebig, M. Albrecht, C. Kloc, O. Gordan, D. R. T. Zahn, S. Michaelis de Vasconcellos, R. Bratschitsch, *Opt. Express* **2013**, *21*, 4908.

[33] C. Jung, S. M. Kim, H. Moon, G. Han, J. Kwon, Y. K. Hong, I. Omkaram, Y. Yoon, S. Kim, J. Park, *Sci. Rep.* **2015**, *5*, 15313.

[34] N. K. Perkgöz, M. Bay, *Nano-Micro Lett.* **2016**, *8*, 70.

[35] R. K. Sharma, G. B. Reddy, *J. Phys. D: Appl. Phys.* **2014**, *47*, 065305.

[36] M. Kastner, *Phys. Rev. Lett.* **1972**, *28*, 355.

[37] A. Anedda, E. Fortin, *J. Phys. Chem. Solids* **1980**, *41*, 865.

[38] Y. Li, A. Chernikov, X. Zhang, A. Rigosi, H. M. Hill, A. M. van der Zande, D. a. Chenet, E.-M. Shih, J. Hone, T. F. Heinz, *Phys. Rev. B* **2014**, *90*, 205422.